Photoproduction of pseudoscalar mesons off nuclei at forward angles

S. Gevorkyan,[1,*] A. Gasparian,[2] L. Gan,[3] I. Larin,[4] and M. Khandaker[5]
[1]*Joint Institute for Nuclear Research, Dubna RU-141980, Russia*
[2]*North Carolina A&T State University, Greensboro, North Carolina 27411, USA*
[3]*University of North Carolina Wilmington, Wilmington, North Carolina 28403, USA*
[4]*Institute for Theoretical and Experimental Physics, Moscow, Russia*
[5]*Norfolk State University, Norfolk, Virginia 23504, USA*
(Received 27 July 2009; published 6 November 2009)

With the advent of new photon-tagging facilities and novel experimental technologies, it has become possible to perform photoproduction cross-sectional measurements of pseudoscalar mesons on nuclei with percent-level accuracy. The extraction of the radiative decay widths from these measurements at forward angles is done by the Primakoff method, which requires theoretical treatment of all processes participating in these reactions at the same percent level. In this work, we review the theoretical approach to meson photoproduction amplitudes in the electromagnetic and strong fields of nuclei at forward angles. The most updated description of these processes are presented based on the Glauber theory of multiple scattering. In particular, the effects of final-state interactions, corrections for light nuclei, and photon shadowing in nuclei are discussed.

DOI: 10.1103/PhysRevC.80.055201 PACS number(s): 25.20.Lj, 11.80.La, 13.60.Le

I. INTRODUCTION

The properties of QCD at low energies are manifested unambiguously in the sector of light pseudoscalar mesons π^0, η, and η'. The two-photon decays of these mesons are primarily caused by the chiral anomaly [1,2], the explicit breaking of a classical symmetry by the quantum fluctuations of the quark fields when they couple to the electromagnetic field. This anomalous symmetry breaking is purely of quantum mechanical origin and can be calculated exactly to all orders in the chiral limit. Particularly, in the case of π^0, which has the smallest mass in the hadron spectrum, higher order corrections are predicted to be small and can be calculated with subpercent accuracy [3–5]. As a result, the precision measurement of the $\pi^0 \to \gamma\gamma$ decay width is widely recognized as an important test of QCD. However, the system of π^0, η, and η' contains fundamental information on the effects of SU(3) and isospin symmetry breaking by the light quark masses. The two-photon decay widths of η and η' have a significant impact on the knowledge of the quark-mass ratio $(m_d - m_u)/m_s$ [6] and the η-η' mixing angle. Precision measurements of the two-photon decay widths of these pseudoscalar mesons thus will provide important inputs for a more accurate understanding of low-energy QCD.

With the recent availabilities of high-energy and high-precision intense photon tagging facilities [7], together with the novel developments in electromagnetic calorimetry, it is feasible to perform percent-level differential cross-sectional measurements of photoproduction of light pseudoscalar mesons π^0, η, and η' on nuclei [8–11]. The two-photon decay widths of these mesons can be extracted from these experiments at forward angles using the Primakoff method [12], in which production of these mesons in the Coulomb field of nuclei is assumed. However, the production process may also be manifested by the exchange of vector mesons that have the same quantum numbers as the photon. The angular distributions of these two production mechanisms are realized differently in the cross sections. The Primakoff production is very sharply peaked at forward angles (0.02° at $E_\gamma \sim 5$ GeV) with practically vanishing strength at a few degrees. The strong production is small under the Primakoff peak, but it begins to dominate at a few degrees. The interference of these two coherent amplitudes with its significant magnitude under the Primakoff peak makes the extraction of the decay widths with high accuracy a difficult task. The full theoretical description of this process, in addition to the two mechanisms previously described, requires correct treatment of the final-state interactions (FSIs) of the produced mesons in nuclear matter, as well as an accounting of incoherent processes. This is necessary to obtain percent-level extraction of the decay widths from experimental data. In this article, we present more general, and perhaps more complete, theoretical descriptions of these photoproduction mechanisms in nuclei. We focus on the example of π^0 production, keeping in mind that the presented results can be extended to η and η' production with appropriate replacements of the parameters and cross sections.

In 1951, Primakoff [12] first proposed measuring the π^0 lifetime from its photoproduction in the Coulomb field of a heavy nucleus (Fig. 1). With that, we consider coherent photoproduction of pseudoscalar mesons on a nucleus at high energies:

$$\gamma + A \to P + A; \quad P = \pi^0, \eta, \eta'. \tag{1}$$

As mentioned, the main challenge in obtaining the π^0 lifetime in this way is related to the presence of the strong amplitude in the photoproduction process (Fig. 2). The full amplitude of this coherent process can be described as a sum

*gevs@jlab.org; on leave of absence from the Yerevan Physics Institute.

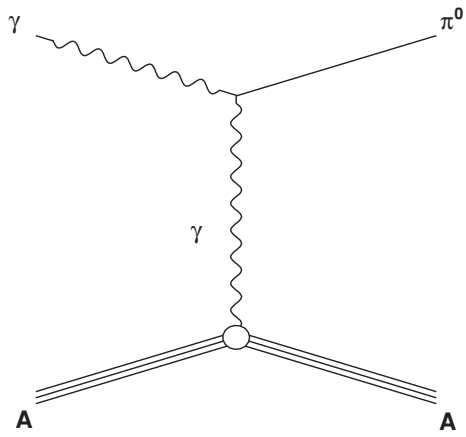

FIG. 1. Pion photoproduction in the nuclear Coulomb field.

of the Coulomb, T_C, and the strong, T_S, parts:

$$T = T_C + e^{i\varphi} T_S, \tag{2}$$

where φ is the relative phase between the Coulomb and the strong amplitudes. By taking into account the incoherent processes, the differential cross section can be expressed as

$$\frac{d\sigma}{d\Omega} = \frac{k^2}{\pi}\frac{d\sigma}{dt} = |T_C + e^{i\varphi} T_S|^2 + \frac{d\sigma_{\rm inc}}{d\Omega}, \tag{3}$$

where $\frac{d\sigma_{\rm inc}}{d\Omega}$ is the incoherent cross section, that is, processes involving excitation or breakup of the target nucleus. Each of these amplitudes factorizes into a photoproduction amplitude on a nucleon multiplied by a corresponding form factor. In addition, these form factors must be modified for the FSIs of the outgoing mesons with nucleons. Interaction of incident high-energy photons with nuclear matter gives rise to a shadowing effect, which has to be considered as well.

II. PHOTOPRODUCTION IN THE COULOMB FIELD OF A NUCLEUS

The effect of the pion FSI in nuclei was first discussed in detail by Morpurgo [13], who considered absorption of the produced pions in the strong nuclear field using the distorted-wave impulse approximation (DWIA). Calculations of the electromagnetic and strong form factors in Ref. [13] have been done with the uniform nuclear-density distribution $\rho(r)$. Based on these assumptions, part of the correction to the strong and electromagnetic form factors, which takes into account pion absorption in nuclei, is correctly obtained. However, the effect of pion rescattering to forward angles was not taken into account. This effect is important for the precise extraction of the decay widths because pions initially produced at modest angles can rescatter to small angles. This effect was first considered by Fäldt [14] in nondiffractive production processes on nuclei in the framework of the Glauber theory of multiple scattering [15]. A general expression (Eq. (3.2) in Ref. [14]) for the electromagnetic amplitude was obtained [14], but an analytically integrable formula was derived for the case of equal absorption in a nucleus of the incident and the produced particles only (Eq. (3.4) in Ref. [14]), which is not the case for the photoproduction processes.

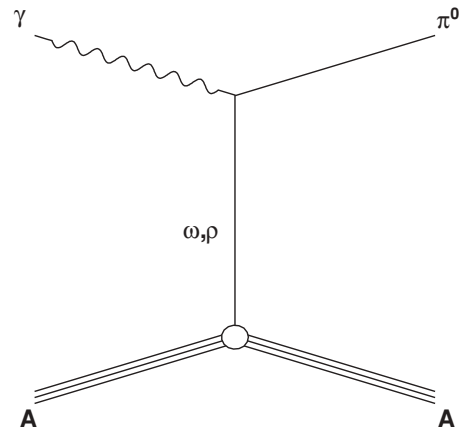

FIG. 2. Pion photoproduction in the strong field of a nucleus.

A. Electromagnetic form factor

In a more general case, based on Glauber multiple-scattering theory and using the independent-particle model for nucleons, the Coulomb amplitude of the photoproduction of mesons on nuclei can be expressed as [13,14]

$$T_C = Z\sqrt{8\alpha\Gamma}\left(\frac{\beta}{m_\pi}\right)^{3/2}\frac{k^2\sin\theta}{q^2+\Delta^2}F_{\rm em}(q,\Delta), \tag{4}$$

where the electromagnetic (em) form factor is given by [16]

$$F_{\rm em}(q,\Delta) = \frac{q^2+\Delta^2}{q}\int J_1(qb)\frac{bd^2bdz}{(b^2+z^2)^{3/2}}e^{i\Delta z} \times \exp\left[-\frac{\sigma'}{2}\int_z^\infty \rho(b,z')dz'\right] \times \int_0^{\sqrt{b^2+z^2}} x^2\rho(x)\,dx, \tag{5}$$

with the following notation:

$$\sigma' = \sigma\left(1 - i\frac{\Re f(0)}{\Im f(0)}\right) = \frac{4\pi}{ik}f(0).$$

Here σ is the πN total cross section and $f(0)$ is the $\pi^0 N \to \pi^0 N$ forward amplitude. The invariant momentum transfer is expressed through the two-dimensional transverse momentum $q = |\vec{q}|$ and longitudinal momentum $\Delta : t = -q^2 - \Delta^2 = -4kp\sin^2(\theta/2) - (m_\pi^2/2k)^2$, where $k = |\vec{k}|$ and $p = |\vec{p}|$ are the photon and pion momenta, respectively.

In Eq. (5), $\rho(r)$ is the nuclear density and $J_1(x)$ is the first-order Bessel function [17]. The integration in Eq. (5) goes over impact parameter b, which is the two-dimensional vector in the plane perpendicular to the incident photon direction and the longitudinal coordinate z.

The Coulomb form factor, $F_{\rm em}(q,\Delta)$, acquires an imaginary part as a result of the longitudinal momentum transfer Δ and the presence of the real part of the pion-nucleon elastic forward amplitude in the absorption process.

The main properties of the Coulomb production are that it rises from zero at a 0° angle and reaches its maximum at

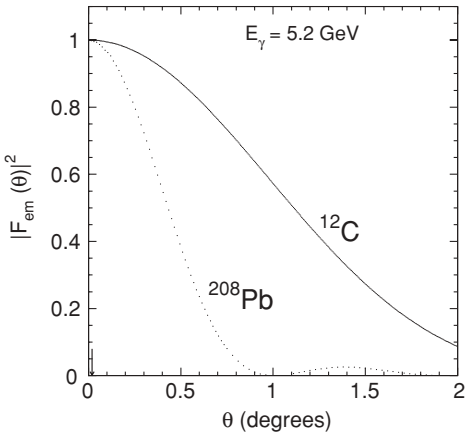

FIG. 3. Square of the electromagnetic form factor for carbon (solid line) and lead (dotted line). The arrow at $\theta_\pi = 0.02^\circ$ indicates the location of the Primakoff peak for the two nuclei.

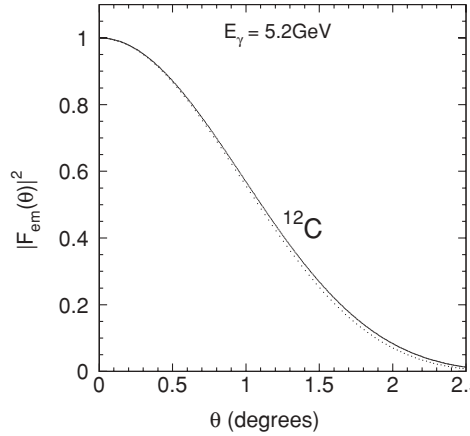

FIG. 4. Square of the electromagnetic form factor for carbon calculated using Eqs. (5) (solid line) and (6) (dotted line).

$q = \Delta = m_\pi^2/2k$ with the specific energy dependence at the peak of $\frac{d\sigma}{dt} \sim k^2$. These properties allow one to separate the Coulomb production (Primakoff process) from the competing nuclear production in the strong field of nuclei, which peaks at relatively large production angles.

For illustration, Fig. 3 shows the angular dependence of the form factors calculated by Eq. (5) for carbon and lead nuclei at 5.2-GeV incident photon energy. In this calculation, the nuclear density $\rho(r)$ was parametrized by Fourier-Bessel analysis from electron-scattering data [18,19]. As evident, the FSI effects are emphasized for the heavier nucleus, though these effects are still very small in the Primakoff region at forward angles.

B. Effect of light nuclei

The photoproduction of mesons in the electromagnetic field of light nuclei requires special consideration. Equation (5) was obtained in the optical limit, which is valid for extended nuclear matter (medium and heavy nuclei). Using multiple-scattering theory [15], we obtain the expression for the electromagnetic form factor for light nuclei suitable for numerical calculations [20]:

$$\begin{aligned} F_{\rm em}(q) &= \frac{q^2+\Delta^2}{q}\int J_1(qb)\frac{bd^2bdz}{(b^2+z^2)^{3/2}}e^{i\Delta z} \\ &\quad\times[1-G(b,z)]^{A-1}\int_0^{\sqrt{b^2+z^2}} x^2\rho_{ch}(x)dx, \\ G(b,z) &= \frac{f_s(0)}{ika_s}\int_z e^{-\frac{(\vec{b}-\vec{s}')^2}{2a_s}}\rho(s',z')d^2s'dz' \\ &= \frac{\sigma'}{2a_s}\int_z e^{-\frac{b^2+s'^2}{2a_s}} I_0\left(\frac{bs'}{a_s}\right)\rho(s',z')s'ds'dz'. \end{aligned} \tag{6}$$

Here, $I_0(x)$ is the zero-order Bessel function of imaginary argument [17]. In deriving this expression, the commonly used parametrization [21] for the elastic $\pi N \to \pi N$ amplitude, $f_s(q) = f_s(0)\exp(-a_s q^2/2)$, was adopted.

For light nuclei such as carbon, the nuclear density, $\rho(r)$, corresponding to the harmonic oscillator potential is widely used in the literature [22]:

$$\rho(r) = \frac{4}{\pi^{3/2}a_0^3}\left(1+\frac{A-4}{6}\frac{r^2}{a_0^2}\right)\exp\left(-\frac{r^2}{a_0^2}\right). \tag{7}$$

The nuclear-charge distribution, $\rho_{\rm ch}(r)$, is obtained by convolution of the nuclear density [Eq. (7)] with the proton's charge distribution. For the latter, we adopt the simple Gaussian parametrization

$$\rho_p(r) = \frac{1}{\pi^{3/2}r_p^3}\exp\left(-\frac{r^2}{r_p^2}\right).$$

Subsequently, the nuclear-charge density can be expressed as[1]

$$\begin{aligned} \rho_{\rm ch}(r) &= \int d^3r'\rho(r')\rho_p(|\vec{r}-\vec{r}'|) \\ &= \frac{2}{\pi^{3/2}\left(a_0^2+r_p^2\right)^{3/2}} \\ &\quad\times\left[1+\frac{(Z-2)}{3}\left(\frac{3r_p^2}{2\left(a_0^2+r_p^2\right)}+\frac{a_0^2r^2}{\left(a_0^2+r_p^2\right)^2}\right)\right] \\ &\quad\times\exp\left(-\frac{r^2}{r_p^2+a_0^2}\right). \end{aligned} \tag{8}$$

Figure 4 shows the difference between the two approaches, Eqs. (5) and (6), in calculating the electromagnetic form factor for the carbon nucleus. The parameters used in these calculations were as follows: proton radius $r_p = 0.8$ fm and an oscillator parameter in Eq. (7) of $a_0 = 1.65$ fm. The form factor calculated by the light nuclei approach [Eq. (6)] falls faster at relatively large angles than the one based on the optical limit. Again, the difference between these two methods in the Primakoff region is practically negligible.

[1]The nuclear density, Eq. (7), is normalized to the atomic number $\int \rho(r)d^3r = A$, whereas the charge density, Eq. (8), is normalized to the number of protons, Z.

C. Nuclear excitation by Coulomb exchange

In addition to the coherent photoproduction in the Coulomb field, production of pions with a nuclear collective excitation (for instance, the giant dipole resonance) is also possible. Such processes were first discussed in Ref. [23], where the following approximation was obtained for the inelastic form factor:

$$|F_n(q)|^2 \approx \frac{1.4N}{2m_p ZAE_{\rm av}}|t|, \tag{9}$$

where m_p and $E_{\rm av}$ are the proton mass and the average excitation energy, respectively, of the nucleus having Z protons and N neutrons. The longitudinal momentum transfer in the case of π^0 photoproduction with nuclear collective excitation is much larger than in the coherent photoproduction: $\Delta_{\rm in} = \Delta + E_{\rm av} \gg \Delta$. Using the fact that the ratio of the "inelastic" to the "elastic" cross sections of the π^0 photoproduction in the Coulomb field as follows:

$$R = \frac{d\sigma_{\rm in}/d\Omega}{d\sigma_{\rm el}/d\Omega} \approx \frac{(q^2+\Delta^2)^2}{\left(q^2+\Delta_{\rm in}^2\right)^2}\frac{|F_n(q)|^2}{|F(q)|^2} \approx \frac{1.4N}{2m_p ZAE_{\rm av}}\frac{(q^2+\Delta^2)^2}{\left(q^2+\Delta_{\rm in}^2\right)}. \tag{10}$$

For the carbon nucleus, the average collective excitation energy is approximately $E_{\rm av} \sim 20$–25 MeV, which, if we use Eq. (10), leads to $R \sim 10^{-7}$ in the Coulomb peak region ($q = \Delta = m_\pi^2/2k$). Thus, the contribution from the nuclear collective excitations can be safely neglected for incident photon energies greater than 1 GeV.

III. COHERENT PHOTOPRODUCTION IN THE STRONG FIELD OF NUCLEI

A. Strong amplitude T_S

The main impact on the lifetime extraction from the measured differential cross sections comes from our knowledge of the strong amplitude T_S in the coherent process of the reaction:

$$\gamma + A \to \pi^0 + A. \tag{11}$$

In the Glauber theory of multiple scattering, this coherent photoproduction amplitude is given by [14]

$$T_S(q,\Delta) = \frac{ik}{2\pi}\int e^{i(\vec{q}\cdot\vec{b}+\Delta z)}\Gamma_p(\vec{b}-\vec{s})\rho(\vec{s},z) \times \left[1-\int \Gamma_s(\vec{b}-\vec{s}')\rho(\vec{s}',z')d^2s'dz'\right]^{A-1} \times d^2bd^2sdz. \tag{12}$$

The two-dimensional vectors $\vec{b}$ and $\vec{s}$ are the impact parameter and the nucleon coordinate in the plane transverse to the incident photon momentum; z is the longitudinal coordinate of the nucleon in the nucleus. The profile functions $\Gamma_{p,s}(\vec{b}-\vec{s})$ are the two-dimensional Fourier transforms of the non-spin-flip elementary amplitudes for the pion photoproduction off the nucleon, $f_p = f(\gamma + N \to \pi^0 + N)$, and elastic pion-nucleon scattering, $f_s = f(\pi + N \to \pi + N)$:

$$\Gamma_{p,s}(\vec{b}-\vec{s}) = \frac{1}{2\pi ik}\int e^{i\vec{q}\cdot(\vec{b}-\vec{s})}f_{p,s}(q)d^2q. \tag{13}$$

Because the slope of the elementary amplitude, $f_s(q)$, is typically much less than the square of the nuclear radii for medium and heavy nuclei, the nuclear density $\rho(r)$ varies slower than the elastic profile functions $\Gamma_s(\vec{b}-\vec{s})$. With this approximation, it is safe to take the $\rho(r)$ outside the integral sign, which leads to

$$\int \Gamma_s(\vec{b}-\vec{s})\rho(s,z)d^2sdz = \frac{\sigma'}{2}\int \rho(\vec{b},z)dz. \tag{14}$$

With special care, the same procedure can also be applied to the production amplitudes [14].

By isolating part of the production amplitude near 0°, $f_p(q) = (\vec{h}\cdot\vec{q})\phi(q)$ [where $\vec{h} = [\vec{k}\times\vec{\epsilon}]/k$, ϵ is the photon polarization vector, and $\phi(0) \neq 0$], we obtain

$$\int \Gamma_p(\vec{b}-\vec{s})\rho(s,z)d^2sdz = \frac{2\pi}{k}\phi(0)\vec{h}\cdot\int\frac{\partial\rho(\vec{b},z)}{\partial\vec{b}}dz. \tag{15}$$

As a result, Eq. (12) can be written in the factorized form

$$T_S(q) = (\vec{h}\cdot\vec{q})\phi(0)F_{\rm st}(q,\Delta),$$
$$F_{\rm st}(q,\Delta) = -\frac{2\pi}{q}\int J_1(qb)\frac{\partial\rho(b,z)}{\partial b}bdbdze^{i\Delta z} \times \exp\left[-\frac{\sigma'}{2}\int_z^\infty \rho(b,z')dz'\right]. \tag{16}$$

The strong form factor, $F_{\rm st}(q,\Delta)$, can be expressed as a sum of two terms, as done in Ref. [14]:

$$F_{\rm st}(q,\Delta) = \int e^{i\vec{q}\cdot\vec{b}}\rho(b,z)d^2bdze^{i\Delta z} \times \exp\left[-\frac{\sigma'}{2}\int_z^\infty \rho(b,z')dz'\right] - \frac{\pi\sigma'}{q} \times \int J_1(qb)\rho(b,z_1)\frac{\partial\rho(b,z_2)}{\partial b}bdbdz_1dz_2e^{i\Delta z_1} \times \exp\left[-\frac{\sigma'}{2}\int_{z_1}^\infty \rho(b,z')dz'\right]. \tag{17}$$

The first term is the usual nuclear form factor and the second one is a correction first introduced by Fäldt [14]. The contribution from the second term is positive (because $[\partial\rho(b,z)]/\partial b < 0$) and can be interpreted as a result of the FSIs of the pions produced in the coherent process at nonzero angles, which (after multiple scattering) come to the forward direction. Note that this correction was obtained [14], as in the case of the electromagnetic part, under the assumption that the cross sections for the incident and produced particles are equal. We have considered a more general case for the photoproduction reactions, and the results are discussed in the following sections.

B. Photon shadowing in nuclei

Real photons at high energies are shadowed in nuclei [21]. Photon shadowing in pion photoproduction is a result of

the two-step process [24]: The initial photon produces a vector meson in the nucleus, which subsequently produces the pseudoscalar meson on another nucleon in the same nucleus. The main contribution to this process comes from the ρ mesons, as the cross section for ρ photoproduction from a nucleon is almost one order of magnitude greater than that for ω production. In addition, the reaction $\omega + N \to \pi^0 + N$ is mainly caused by isospin-one exchange (ρ exchange), and the production amplitudes on protons and neutrons have different signs. Because the nuclear coherent amplitude is a sum over the elementary photoproduction amplitudes, the ω contribution gets an additional suppression.

Using multiple-scattering techniques, one can obtain the contribution from the intermediate ρ channel to the strong form factor:

$$F_I(q) = -\frac{\pi\sigma'}{q}\int J_1(qb)\rho(b,z_1)\frac{\partial\rho(b,z_2)}{\partial b} \times \theta(z_2-z_1)bdbdz_1dz_2e^{i\Delta_\rho(z_1-z_2)+i\Delta z_2} \times \exp\left[-\frac{\sigma'}{2}\int_{z_1}^{\infty}\rho(b,z')dz\right], \tag{18}$$

where $\Delta_\rho = m_\rho^2/2E$ is the longitudinal momentum transfer in the ρ meson photoproduction off the nucleon. The strong amplitude accounting for the photon shadowing reads

$$T_S(q) = (\vec{h}\cdot\vec{q})\phi(0)(F_{\rm st} - wF_I), \qquad w = \frac{f(\gamma N\to\rho N)f(\rho N\to\pi N)}{f(\rho N\to\rho N)f(\gamma N\to\pi N)}, \tag{19}$$

where the range of the shadowing parameter w is between 0 (no shadowing) and 1 (vector dominance model, VDM).

Equation (18) and Fäldt's correction [the second term in Eq. (17)] are very similar, and the only difference is in the energy dependence through the longitudinal momentum transfer. It is interesting to mention here that at high energies where $\Delta = \Delta_\rho = 0$, assuming validity of the naive VDM ($w = 1$), the two terms cancel each other. Thus, the strong form factor is determined only by the first term in Eq. (17). In this limit, the integration over z in Eq. (17) can be done analytically:

$$F_{\rm st}(q) = \frac{2}{\sigma'}\int d^2b e^{i\vec{q}\cdot\vec{b}}\left(1-\exp\left[-\frac{\sigma'}{2}\int\rho(b,z')dz\right]\right). \tag{20}$$

This expression looks very similar to the one for coherent production of pions by ρ mesons, a well-known fact for diffractive processes [21].

The effect of photon shadowing on the strong form factor in Eq. (19) is demonstrated in Figs. 5 and 6 for carbon and lead nuclei, calculated from Eqs. (17)–(19) for two extreme values of the shadowing parameter: $w = 0$ (no shadowing) and $w = 1$ (naive VDM). As shown, the results for both nuclei are strongly dependent on the value of w.

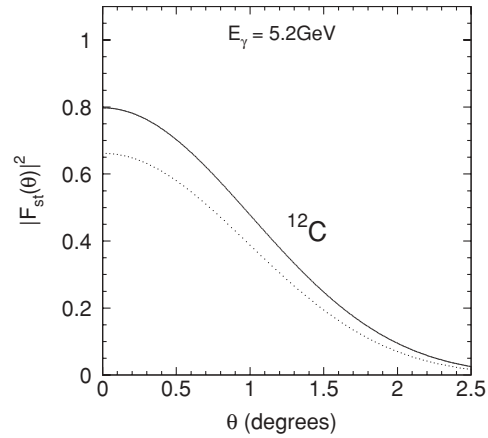

FIG. 5. Square of the strong form factor for carbon without shadowing ($w = 0$, solid line) and with maximal photon shadowing ($w = 1$, dotted line).

C. Two-step contribution in light nuclei

The optical limit approximations, usually used in the literature for these calculations, can potentially lead to a correction for light nuclei that can be critical for the precision extraction of decay width from the experimental cross sections.

For light nuclei, we parametrize the elementary production amplitudes in the following way:

$$f_p = \phi(0)(\vec{h}\cdot\vec{q})\exp\left(-\frac{a_pq^2}{2}\right), \qquad f_s = f_s(0)\exp\left(-\frac{a_sq^2}{2}\right). \tag{21}$$

Here, $\phi(0)$, $f_s(0)$, and a_p, a_s are the forward elementary amplitudes and their relevant slopes, respectively. With these

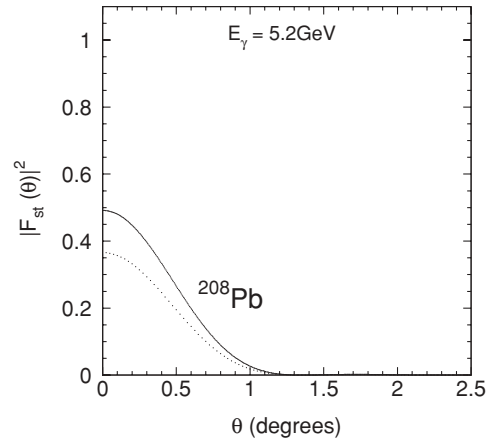

FIG. 6. Square of the strong form factor for lead without shadowing ($w = 0$, solid line) and with maximal photon shadowing ($w = 1$, dotted line).

parametrizations, one obtains

$$\Gamma_p(\vec{b}-\vec{s}) = \frac{\vec{h}\cdot(\vec{b}-\vec{s})}{ka_p^2}\phi(0)\exp\left[-\frac{(\vec{b}-\vec{s})^2}{2a_p}\right],$$
$$\Gamma_s(\vec{b}-\vec{s}) = \frac{f_s(0)}{ika_s}\exp\left[-\frac{(\vec{b}-\vec{s})^2}{2a_s}\right]. \quad (22)$$

By substituting Eq. (22) into Eq. (12), we obtain

$$T_S(q,\Delta) = (\vec{h}\cdot\vec{q})\phi(0)F_{\rm st}(q,\Delta),$$
$$F_{\rm st}(q,\Delta) = \frac{2\pi}{qa_p^2}\int J_1(qb)\left[bI_0\left(\frac{bs}{a_p}\right) - sI_1\left(\frac{bs}{a_p}\right)\right] \times e^{i\Delta z}e^{-\frac{b^2+s^2}{2a_p}}\rho(s,z)[1-G(b,z)]^{A-1}bdbsdsdz$$
$$G(b,z) = \frac{f_s(0)}{ika_s}\int_z e^{-\frac{(\vec{b}-\vec{s}')^2}{2a_s}}\rho(s',z')d^2s'dz' = \frac{\sigma'}{2a_s}\int_z e^{-\frac{b^2+s'^2}{2a_s}}I_0\left(\frac{bs'}{a_s}\right)\rho(s',z')s'ds'dz'. \quad (23)$$

The amplitude relevant to the two-step process $\gamma \to \rho \to \pi^0$ in multiple-scattering theory is given by

$$T_I(q) = \frac{ik}{2\pi}\frac{A-1}{A}\int e^{i\vec{q}\cdot\vec{b}}d^2b\Gamma_{\gamma\rho}(\vec{b}-\vec{s}_1)\Gamma_{\rho\pi}(\vec{b}-\vec{s}_2) \times \rho(s_1,z_1)\rho(s_2,z_2)\theta(z_2-z_1)e^{i[\Delta_\rho(z_1-z_2)+\Delta z_2]} \times [1-G(b,z_1)]^{A-2}d^2s_1d^2s_2dz_1dz_2. \quad (24)$$

where $\Delta_\rho = m_\rho^2/2E$ is the longitudinal momentum transfer in the elementary reaction $\rho + N \to \pi^0 + N$. The relevant form factor can be expressed in a form convenient for numerical integration:

$$F_I(q,\Delta_\rho,\Delta) = \frac{A-1}{A}\frac{\pi\sigma'}{qa_sa_p^2}\int J_1(qb)I_0\left(\frac{bs_2}{a_s}\right) \times \left[bI_0\left(\frac{bs_1}{a_p}\right) - s_1I_1\left(\frac{bs_1}{a_p}\right)\right] \times \theta(z_2-z_1)\rho(s_1,z_1)\rho(s_2,z_2) \times e^{-\frac{(a_p+a_s)b^2}{2a_pa_s}}e^{-(\frac{s_1^2}{2a_p}-\frac{s_2^2}{2a_s})}e^{i[\Delta_\rho(z_1-z_2)+\Delta z_2]} \times [1-G(b,z_1)]^{A-2} \times bdbs_1ds_1s_2ds_2dz_1dz_2. \quad (25)$$

In Fig. 7, the square of the strong form factor for the carbon nucleus, including the intermediate channel corrections, is plotted for two different cases: (a) The solid line is calculated by Eqs. (17)–(19) with the optical model approximations and (b) the dotted line is calculated by multiple-scattering theory for light nuclei without the optical model approximations [using Eqs. (23)–(25)]. The oscillator type of nuclear density [Eq. (7)] and the shadowing parameter $w = 0.25$ [25,26] are used in both calculations. As shown, the fall of the form factor calculated without the optical model approximations (dotted line) is sizeably faster and therefore important for the precise extraction of the decay widths. Similar behavior was observed for the electromagnetic form factor shown in Fig. 4.

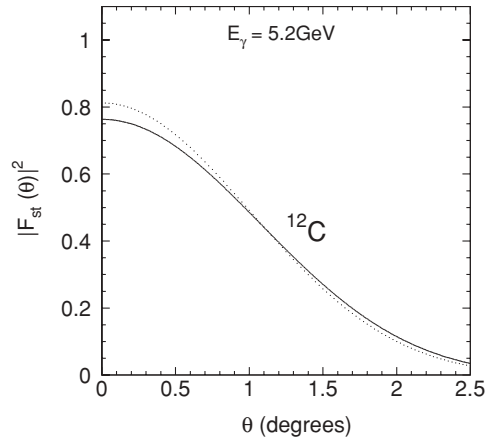

FIG. 7. Square of the strong form factor for carbon nucleus calculated with (solid line) and without (dotted line) the optical model approximations.

IV. INCOHERENT PHOTOPRODUCTION

Incoherent meson photoproduction is a production with the excitation or a breakup of the target nucleus:

$$\gamma + A \to \pi^0 + A'. \quad (26)$$

The general expression for the incoherent cross section established in the literature [27,28] is given by

$$\frac{d\sigma_{\rm inc}}{d\Omega} = \frac{d\sigma_0}{d\Omega}(q)N(0,\sigma)[1-G(t)], \quad (27)$$

where $d\sigma_0/d\Omega$ is the elementary cross section on the nucleon $\gamma + N \to \pi^0 + N$ and

$$N(0,\sigma) = \int \frac{1-e^{-\sigma T(b)}}{\sigma}d^2b. \quad (28)$$

Here, $T(b) = \int \rho(b,z)dz$. The factor $1-G(q)$ takes into account the suppression of pions produced at small angles resulting from the Pauli exclusion principle [27] and goes to 0 at small angles. However, as was shown for the case of the proton scattering on nuclei [22], multiple scattering leads to the incoherent cross section, which is different from 0 at 0 angles. The same effects should also be seen in pseudoscalar meson photoproduction. Assuming that the meson photoproduction cross section on the nucleon is completely determined by the spin-nonflip amplitude, one can parametrize the differential cross section on the nucleon as[2]

$$\frac{d\sigma_0}{d\Omega} = c_pq^2e^{-a_pq^2}. \quad (29)$$

Using this parametrization, we can show[3] that the incoherent cross section of the process under consideration can be

[2]Numerically, this parametrization at small momentum transfer coincides with the predictions for π^0 photoproduction cross section on the proton obtained in the framework of the improved Regge theory [29].

[3]The derivation and detailed discussion of the incoherent production at small angles will be presented elsewhere.

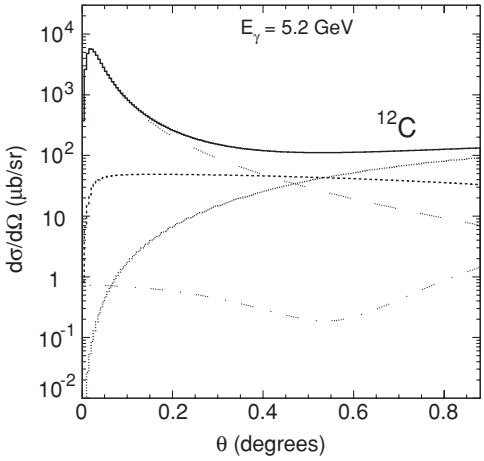

FIG. 8. Differential cross section for π^0 photoproduction off a carbon nucleus as a function of the production angle in the laboratory system. The long-dashed line shows the electromagnetic (Primakoff) contribution; the dotted line is the strong part; the dash-dotted line is the incoherent cross section; the short-dashed line is the interference between the Primakoff and the strong amplitudes; and the solid line is the full cross section.

represented as

$$\frac{d\sigma_{\rm inc}}{d\Omega} = \frac{d\sigma_0}{d\Omega}(q)\left[N(0,\sigma) - \frac{|F_{\rm st}(q)|^2}{A}\right] + c_p e^{-a_p q^2}\xi^2,$$
$$\xi^2 = \left|\frac{\sigma'}{2}\right|^2 \int \rho(b,z)\left|\frac{\partial T(b,z)}{\partial b}\right|^2 \times \exp\left[-\sigma T(b,z)\right] d^2b\,dz. \quad (30)$$

Here, $F_{\rm st}(q)$ is the strong form factor of the nucleus [Eq. (17)]. One can easily see that only in the case when absorption is absent ($\sigma = 0$) does the factorization similar to Eq. (27) take place.

In Fig. 8, we plot the differential cross section for π^0 photoproduction off the carbon nucleus versus the laboratory angle. The different curves give the relevant mechanism as previously discussed. All calculations have been done using the expressions obtained in the present work. The non-spinflip π^0 photoproduction amplitude on the nucleon was parametrized as [30,31] $f(q) = 10\sin\theta(k/k_0)^{1.2}e^{i\varphi}$, where $\varphi \sim 1$ radian [30] and $k_0 = 1$ GeV. The differential cross section of π^0 photoproduction on the proton was taken in accordance with existing experimental data [32] at forward angles.

V. SUMMARY

We have extended the theoretical treatment of photoproduction of pseudoscalar mesons off nuclei at forward angles described in the literature in connection with the extraction of their radiative decay widths. Based on the Glauber theory of multiple scattering, we have derived complete analytical expressions for the electromagnetic and strong form factors specific for the photoproduction of pseudoscalar mesons off both light and heavy nuclei, valid for realistic charge and matter distributions. The electromagnetic form factor for the nondiffractive photoproduction processes is derived for the first time. Special attention is paid to light nuclei, because with increasing photon beam energies, the extraction of decay widths with high precision is becoming more feasible from the light targets. We have included in our results the difference between the charge and matter distributions for the light nuclei. The photon shadowing effect in the reactions under consideration is correctly treated for the first time. The impact of this effect on π^0 meson production in the strong field of both light and heavy nuclei is calculated. An expression for the incoherent photoproduction cross sections of the pseudoscalar mesons at forward angles is derived, which correctly takes into account the mesons' FSIs and the exclusion principle. Using the obtained expressions, we calculate the differential cross section of the π^0 meson photoproduction off the carbon nucleus and the contributions of different mechanisms. All these give a good theoretical foundation to extract the lifetime of pseudoscalar mesons from forthcoming experimental data with high precision.

ACKNOWLEDGMENTS

This work was inspired by the PrimEx experiment at Jefferson Laboratory to measure the π^0 lifetime via the Primakoff effect with high precision. It was partially supported by National Science Foundation Grant Nos. PHY-0245407 and PHY-0555524.

[1] J. S. Bell and R. Jackiw, Nuovo Cimento A **60**, 47 (1969).
[2] S. L. Adler, Phys. Rev. **177**, 2426 (1969).
[3] J. L. Goity, A. M. Bernstein, and B. R. Holstein, Phys. Rev. D **66**, 076014 (2002).
[4] B. Ananthanarayan and B. Moussallam, J. High Energy Phys. 05 (2002) 052.
[5] B. L. Ioffe and A. G. Oganesian, Phys. Lett. **B647**, 389 (2007).
[6] H. Leutwyler, Phys. Lett. **B378**, 313 (1996).
[7] D. I. Sober *et al.*, Nucl. Instrum. Methods A **440**, 263 (2000).
[8] K. Assamagan, L. Gan, A. Gasparian *et al.*, Jefferson Lab. Proposal, PR99-04, http://www.jlab.org/exp_prog/proposals/99prop.html.
[9] A. Ahmidouch, S. Danagulian, A. Gasparian *et al.*, Jefferson Lab. Proposal, PR02-103, http://www.jlab.org/exp_prog/proposals/02prop.html.
[10] A. Gasparian, P. Ambrozewicz, R. Pedroni *et al.*, Jefferson Lab. Proposal, PR08-023, http://www.jlab.org/exp_prog/proposals/08prop.html.
[11] Conceptual Design Report (CDR) for Science and Experimental Equipment for the 12 GeV Upgrate of CEBAF, 6–8 April 2005, http://www.jlab.org/12Gev/development.html.
[12] H. Primakoff, Phys. Rev. **81**, 899 (1951).
[13] G. Morpurgo, Nuovo Cimento **31**, 569 (1964).
[14] G. Fäldt, Nucl. Phys. **B43**, 591 (1972).

[15] R. J. Glauber, in *Proceedings of the Second International Conference, Rehovoth, 1967*, edited by G. Alexander (North-Holland, Amsterdam, 1967), p. 311.
[16] S. Gevorkyan, A. Gasparian, and L. Gan, PrimEx Note 45, 2007, http://www.jlab.org/primex/.
[17] M. Abramowitz and I. Stegun, *Handbook of Mathematical Functions*, NBS Appl. Math. Ser. No. 55 (U.S. GPO, Washington, DC, 1964).
[18] C. W. de Jager, M. de Vries, and C. de Vries, At. Data Nucl. Data Tables **14**, 479 (1974).
[19] E. Offerman, L. S. Cardman, C. W. de Jager, H, Miska, C. de Vries, and H. de Vries, Phys. Rev. C **44**, 1096 (1991).
[20] S. Gevorkyan, I. Larin, A. Gasparian, and L. Gan, PrimEx Note 48, 2007, http://www.jlab.org/primex/.
[21] T. Bauer, R. Spital, D. Yennie, and F. Pipkin, Rev. Mod. Phys. **50**, 261 (1978).
[22] L. R. B. Elton, *Nuclear Sizes* (Oxford University Press, London, 1961).
[23] V. Glaser and R. Ferrell, Phys. Rev. **121**, 886 (1961).
[24] K. Gottfried and D. Yennie, Phys. Rev. **182**, 1595 (1969).
[25] W. Meyer *et al.*, Phys. Rev. Lett. **28**, 1344 (1972).
[26] A. M. Boyarski *et al.*, Phys. Rev. Lett. **23**, 1343 (1969).
[27] C. A. Engelbrecht, Phys. Rev. **133**, B988 (1964).
[28] G. Bellettini *et al.*, Nuovo Cimento A **66**, 243 (1970).
[29] A. Sibirtsev, J. Haidenbauer, S. Krewald, U.-G. Meisner, and A. W. Thomas, Eur. Phys. J. A **41**, 71 (2009).
[30] A. Browman *et al.*, Phys. Rev. Lett. **33**, 1400 (1974).
[31] R. Anderson *et al.*, Phys. Rev. D **4**, 1937 (1971).
[32] M. Braunschweig *et al.*, Nucl. Phys. **B20**, 191 (1970).